Weierstraß-Institut
für Angewandte Analysis und Stochastik
Leibniz-Institut im Forschungsverbund Berlin e. V.

Preprint ISSN 2198-5855

3D electrothermal simulations of organic LEDs showing negative differential resistance

Matthias Liero[1], Jürgen Fuhrmann[1], Annegret Glitzky[1], Thomas Koprucki[1],

Axel Fischer[2], Sebastian Reineke[2]

submitted: September 1, 2017

[1] Weierstrass Institute
Mohrenstr. 39
10117 Berlin
Germany
E-Mail: matthias.liero@wias-berlin.de
juergen fuhrmann.liero@wias-berlin.de
annegret.glitzky@wias-berlin.de
thomas.koprucki@wias-berlin.de

[2] Dresden Integrated Center for Applied Physics and Photonic Materials (IAPP)
TU Dresden
Nöthnitzer Str. 61
01187 Dresden
Germany
E-Mail: axel.fischer@iapp.de
sebastian.reineke@iapp.de

No. 2420
Berlin 2017

2010 *Mathematics Subject Classification.* 35Q79, 35J92, 80M12.

2008 *Physics and Astronomy Classification Scheme.* 72.20.Pa, 72.80.Le, 81.05.Fb, 85.80.Fi, 02.60.Cb.

Key words and phrases. Organic semiconductors, self-heating, negative differential resistance, p-Laplacian, thermistor model, hybrid finite-volume/finite-element scheme.

This work received funding via the Research Center Matheon supported by ECMath in projects D-SE2 and D-SE18, the DFG CRC 787 ”Semiconductor Nanophotonics”, and it was supported in part by the DFG within the Cluster of Excellence Center for Advancing Electronics Dresden (cfaed) and the DFG project EFOD (RE 3198/6-1).

Edited by
Weierstraß-Institut für Angewandte Analysis und Stochastik (WIAS)
Leibniz-Institut im Forschungsverbund Berlin e. V.
Mohrenstraße 39
10117 Berlin
Germany

Fax: +49 30 20372-303
E-Mail: preprint@wias-berlin.de
World Wide Web: http://www.wias-berlin.de/

3D electrothermal simulations of organic LEDs showing negative differential resistance

Matthias Liero, Jürgen Fuhrmann, Annegret Glitzky, Thomas Koprucki,
Axel Fischer, Sebastian Reineke

Abstract

Organic semiconductor devices show a pronounced interplay between temperature-activated conductivity and self-heating which in particular causes inhomogeneities in the brightness of large-area OLEDs at high power. We consider a 3D thermistor model based on partial differential equations for the electrothermal behavior of organic devices and introduce an extension to multiple layers with nonlinear conductivity laws, which also take the diode-like behavior in recombination zones into account. We present a numerical simulation study for a red OLED using a finite-volume approximation of this model. The appearance of S-shaped current-voltage characteristics with regions of negative differential resistance in a measured device can be quantitatively reproduced. Furthermore, this simulation study reveals a propagation of spatial zones of negative differential resistance in the electron and hole transport layers toward the contact.

1 Introduction

The charge carrier transport in optoelectronic devices based on organic materials is realized by temperature activated hopping between adjacent molecules, cf. [BK11]. In connection with Joule self-heating this leads to a strong positive feedback between power dissipation, temperature, conductivity, and current flow and results in complicated nonlinear behavior such as S-shaped current-voltage relations including regions of negative differential resistance (NDR) and hysteresis phenomena, see [FPL$^+$13]. There, the electrothermal behavior of organic semiconductors was described by a homogeneous thermistor model for the total current flow coupled to a global heat balance. This model was extended in [FKG$^+$14] by considering spatially resolved electrothermal circuit models to explain the brightness inhomogeneities in large-area OLEDs at high power. In particular, the circuit model reproduced the experimentally observed S-shaped NDR behavior. Motivated by this successful approach, a thermistor model based on partial differential equations (PDEs) was introduced in [LKF$^+$15], which offers more flexibility with respect to device geometries and material variations.

In the present paper, we introduce an extension of this PDE-based thermistor model by including more complex nonlinear conductivity laws and the diode-like behavior of recombination zones (see Section 2). The numerical approximation and its implementation in a simulation tool is based on the hybrid finite-volume/finite-element scheme discussed in [FGL17] and is briefly summarized in Section 3. For our simulation study we consider a 2.54 mm $\times$ 2.54 mm red OLED manufactured at TU Dresden as described in Section 4. The resulting current densities and temperature distributions as well as the current-voltage characteristics are presented in Section 5 together with a comparison to measurements.

DOI 10.20347/WIAS.PREPRINT.2420 Berlin 2017

2 PDE thermistor model for current and heat flow

In [LKF+15] the following 3D PDE model was developed to describe the interplay of current and heat flow in OLEDs. It consists of a current flow equation for the electrostatic potential φ and a heat equation for the temperature T

$$\begin{aligned} -\nabla\cdot(\sigma(x,T,|\nabla\varphi|)\nabla\varphi) &= 0 && \text{in } \Omega_{\rm el}\subset\Omega_{\rm heat},\\ -\nabla\cdot(\lambda(x)\nabla T) &= H(x,T,|\nabla\varphi|) && \text{in } \Omega_{\rm heat} \end{aligned} \tag{1}$$

with electrical conductivity σ, heat conductivity λ, and Joule heat term H. In general, the spatial domain $\Omega_{\rm el}$ covers all electrically active regions (electrodes, OLED stack) whereas $\Omega_{\rm heat}$ may additionally contain parts of the substrate and the surrounding.

The special features of this model are a temperature dependence of the conductivity function σ according to an Arrhenius-like law as well as a non-Ohmic current-voltage relation incorporated by a power law, namely

$$\sigma(x,T,|\nabla\varphi|)=\sigma_0(x)F(x,T)\Big|\frac{|\nabla\varphi|}{E_{\rm ref}}\Big|^{p(x)-2},\ F(x,T)=\exp\Big[-\frac{E_{\rm a}(x)}{k_{\rm B}}\Big(\frac{1}{T}-\frac{1}{T_{\rm a}}\Big)\Big].$$

Here, $T_{\rm a}>0$ and $k_{\rm B}$ denote the fixed ambient temperature and Boltzmann's constant. The quantitites σ_0, p, and $E_{\rm a}$ are the material dependent reference conductivity, power law exponent, and activation energy, respectively, which have to be extracted from measurements, from drift-diffusion or Monte Carlo simulations. The exponent $p(x)$ takes different power laws in the various layers of the device into account. The current flow equation becomes of $p(x)$-Laplacian type with discontinuous but piecewise constant exponent p. In particular, in Ohmic materials such as electrodes we have $p(x)\equiv 2$ and different values $p(x)>2$ in organic layers (comp. Table 1).

In $\Omega_{\rm el}$, the Joule heat term in the heat equation takes the form

$$H(x,T,|\nabla\varphi|)=(1-\eta(x,T,|\nabla\varphi|))\sigma_0(x)F(x,T)|\nabla\varphi|^{p(x)},$$

where $\eta(x,T,|\nabla\varphi|)\in[0,1]$ represents the light-outcoupling factor. Outside it vanishes.

The system is complemented by Dirichlet boundary conditions for the potential φ at the contacts Γ_D and no-flux boundary conditions at the insulating parts Γ_N of the boundary $\partial\Omega_{\rm el}$; the heat flow into the environment is decribed by Robin boundary conditions:

$$\begin{aligned} &\varphi=\varphi^D \text{ on } \Gamma_D, \qquad \sigma(x,T,|\nabla\varphi|)\nabla\varphi\cdot\nu=0 \text{ on } \Gamma_N,\\ &-\lambda(x)\nabla T\cdot\nu=\gamma(x)(T-T_{\rm a}) \text{ on } \Gamma=\partial\Omega_{\rm heat}. \end{aligned} \tag{2}$$

Since the Joule heat term H is less regular (a priori only in L^1), the mathematical treatment of the system is not straightforward. The existence, boundedness and the regularity of solutions to Problem (1), (2) has been investigated in [BGL16, GL17].

Here, we extend this model by considering different parallel running transport mechanisms in various substructures realized by an electrical conductivity of the form

$$\sigma(x,T,|\nabla\varphi|)=\sum_{i=0}^{N}\sigma_i(x)\exp\Big[-\frac{E_{{\rm a},i}(x)}{k_{\rm B}}\Big(\frac{1}{T}-\frac{1}{T_{\rm a}}\Big)\Big]\Big|\frac{|\nabla\varphi|}{E_{\rm ref}}\Big|^{p_i(x)-2}.$$

In particular, charge transport processes with different values of the activation energy $E_{\rm a}$ and operating with different power law exponents can be included. Moreover, we account for the diode-like behavior

of OLEDs by an exponential law for the conductivity only in the recombination zones (see Fig. 1)

$$\sigma_{\mathrm{reco}}(x,T,|\nabla\varphi|) = i_0 F(x,T)\Big(\exp\frac{lq|\nabla\varphi|}{nk_{\mathrm{B}}T} - 1\Big)\frac{1}{|\nabla\varphi|} \tag{3}$$

with saturation current i_0, ideality factor n, characteristic length l, and elementary charge q.

3 Numerical method for solving the 3D thermistor model

Our approximation of the PDE thermistor model (1), (2) is realized by a hybrid finite-volume/finite-element scheme that is introduced in [LKF$^+$15] and discussed in more detail in [FGL17]. Since for OLED structures, the exponent p is a piecewise constant function, we subdivide the computational domain $\overline{\Omega} = \bigcup_{r\in\mathcal{R}} \overline{\Omega}_r$ into disjoint subdomains given by the regions of continuity of the coefficients, cf. Fig. 1 (left) and call the common boundary between two neighboring regions hetero interface.

Due to its ability to preserve the maximum principle for the current flow equation and the positivity of the temperature, we chose a two-point flux finite-volume method for the discretization of (1), (2). Our control volumes are Voronoi cells based on a boundary conforming Delaunay grid with respect to boundaries and hetero interfaces. We apply Gauss theorem to substitute the divergence of the fluxes on Voronoi control volumes by contributions of the normal fluxes over the faces of the control volumes. Since the electrical conductivity depends on the full gradient $|\nabla\varphi|$, we approximate $\nabla\varphi$ here by suitable averages of P1 finite element gradients, see [FGL17, Section 4] for a discussion of the arising difficulties. The technique proposed in [BH08] allows to evaluate the Joule heat approximation by edge contributions. In particular, this approximation scheme enables us to treat the exponential law (3) for the conductivity in recombination zones. Note that for thin-film devices our discretization scheme reflects exactly the Kirchhoff laws in circuit models as used in [FKG$^+$14].

This discretization approach leads to nonlinear systems of algebraic equations which need to be solved for each applied bias. For this purpose, we use a Newton method with full analytical Jacobians in combination with a sparse direct solver.

However, the straightforward simulation of devices with S-shaped current-voltage relation and regions of NDR by variation of the terminal voltages leads to singular Jacobi matrices at the inflection points of the S-shaped characteristics. A path-following technique realized by a predictor-corrector method as described in [FGL17] remedies this situation and allows to track the unstable parts of the current-voltage curve. The implementation is done on the basis of the software package WIAS-pdelib.

4 Simulation setup for OLED test samples

We apply our PDE thermistor model and the related simulation tool to describe the electrothermal behavior of OLED samples prepared and experimentally investigated at TU Dresden. We consider a quadratic 2.54 mm $\times$ 2.54 mm red emitting OLED (see Fig. 1 left) deposited on a glass substrate. In the stack, the transparent cathode, enabling top light emission, is formed by thin layers of Ag and Au and contacted from the left side. Due to the much higher electrical conductivity of the opaque anode (bottom contact) we replace the current flow equation in the anode by imposing a Dirichlet boundary condition at the upper boundary of the bottom electrode. The computational domain Ω_{heat} for the heat equation covers the OLED stack and a 6.54 mm $\times$ 6.54 mm part of the 1.1 mm thick glass substrate. The influence of the remaining substrate is described by boundary conditions. By symmetry

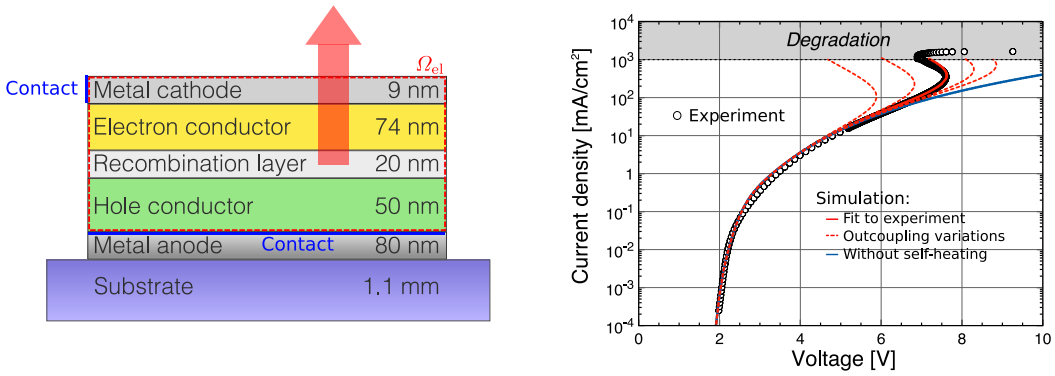

Figure 1: Left: Schematic cross-section of the simulated OLED stack. The transparent cathode is formed by 7 nm Ag on 2 nm Au as described in [SSMM+13]. The electron conductor consists of TPBi:Cs and Balq2 layers, the emissive layer is Spiro-TAD:Ir(MDQ)$_2$(acac), the hole conductor is made of Spiro-TAD and a Spiro-TTB:$C_{60}F_{36}$ layer, and the bottom anode is formed by 40 nm Ag on Al 40 nm. Right: Simulated and measured S-shaped current-voltage relations with regions of NDR for different thermal outcoupling regimes realized by different values of the outcoupling coefficient γ in (2).

Table 1: Material parameters

Layer	σ_0 [S/cm]	$E_{a,0}$ [meV]	p	σ_1 [S/cm]	$E_{a,1}$ [meV]	η	λ [W/m/K]
n-system	2.51×10^{-8}	325	4.07	1.19×10^{-8}	475	0.0	0.4
p-system	5.67×10^{-8}	200	4.7	1.19×10^{-8}	270	0.0	0.4
cathode	7.41×10^{-6}	0	2.0	0	0	0.0	300

arguments, only half of the structure has to be simulated. The voltage is increased at the top contact, and the potential is fixed to 0 at the bottom electrode.

The ambient temperature is set to $T_a = 293$ K, in the glass substrate and the anode we assume heat conductivities λ of 1.8 W/m/K and 300 W/m/K, respectively. For the recombination layer we use $\lambda = 0.4$ W/m/K and the exponential law (3) with the parameters $i_0 = 4.8 \times 10^{-23}$ A/m^2, $E_{a,0} = 1.588$ eV, $l = 20$ nm, $n = 1.7$, $\eta = 0.2$. The material parameters for the electron transport layer (n-system), hole transport layer (p-system) and the top cathode are collected in Table 1. These parameters are obtained from the analysis of a simplified homogeneous model. The details of the experimental parameter estimation and possibly improved parameters are subject of a future publication.

5 Discussion of simulation results

For the geometry and material parameters described above 3D simulations of the OLED structure have been performed. For the heat transfer through the top boundary a fixed $\gamma = 10$ W/(m^2·K) was used, whereas for the remaining boundary the values 10, 40, 110, 200, and 600 (in W/(m^2·K)) for γ were chosen to model different thermal coupling conditions. Fig. 1 (right) compares measured with simulated current-voltage curves. For $\gamma = 110$ W/(m^2·K), the simulation accurately describes the experimentally obtained S-shaped current-voltage characteristics including the region of NDR. Self-heating effects are clearly visible at 6 V ($I = 30$ mA/cm^2). We emphasize, that other PDE modeling approaches for the electrothermal behavior in organic LEDs are available, see [SBH+11, KAH+17].

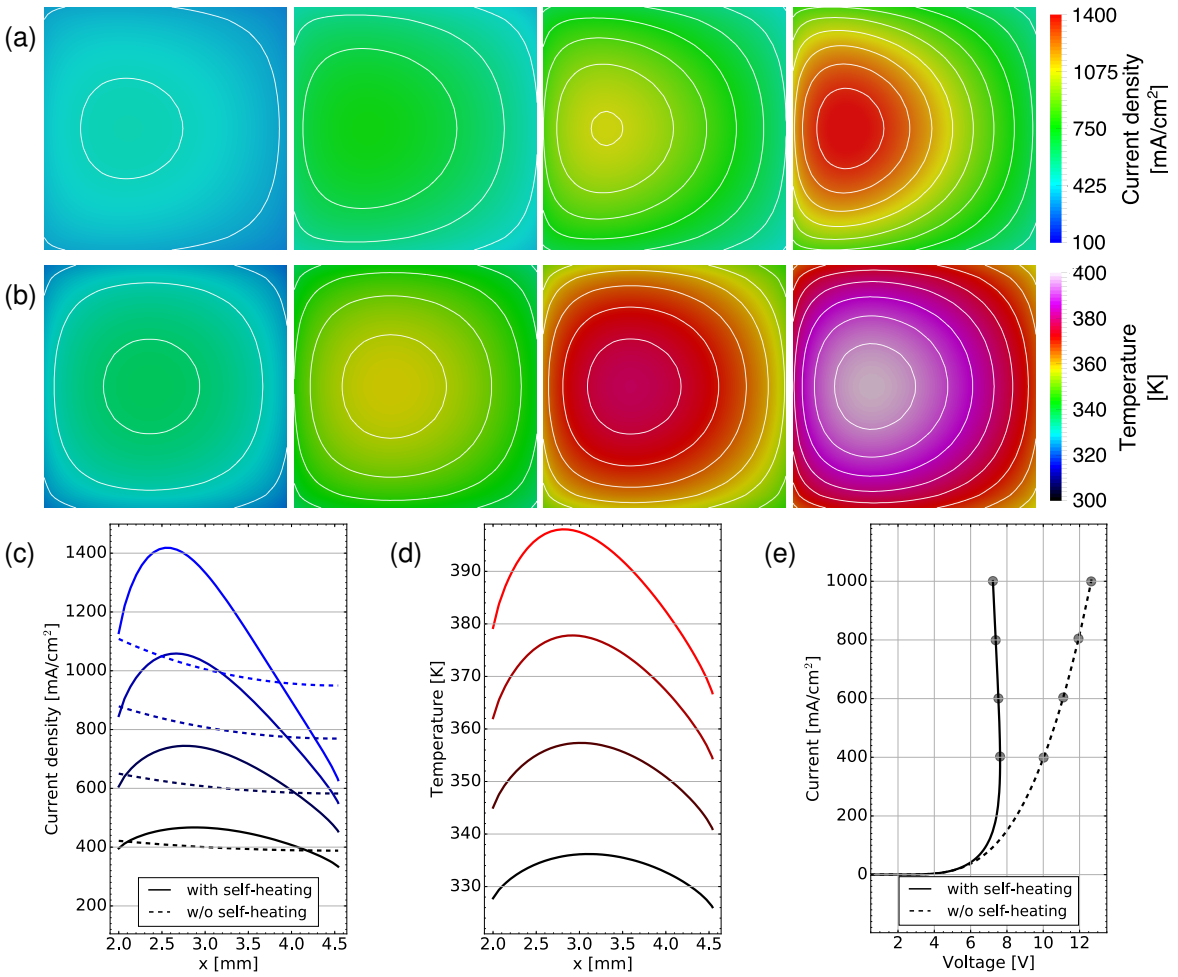

Figure 2: a) Simulated inhomogeneous current density and b) temperature distribution in a horizontal cross section of the OLED stack at values of an average current density (total current over anode devided by anode area) of 400, 600, 800, and 1000 mA/cm^2. c) Values for current density and temperature at cut along symmetry line of the horizontal cross-section, dashed lines correspond to the isothermal case where self-heating is neglected, d) shows corresponding temperature distribution. e) Self-consistent current-voltage characteristics in comparison to the isothermal one.

However, a S-shaped characteristics and NDR phenomena are not reported therein. In particular, in [KAH$^+$17] the temperature dependence of the conductivity is neglected such that only a one-way coupling is considered. In contrast, our model takes the self-heating self-consistently into account and is able to properly describe the feature of S-shaped characteristics with NDR regions.

The value of the turnover voltage is 7.62 V ($I = 398\,\mathrm{mA/cm^2}$). Material degradation sets in at $I = 1\,\mathrm{A/cm^2}$ corresponding to a maximal temperature value of the simulation of around 398 K. This value is in good agreement with experiments of externally heated samples as it will be shown elsewhere.

Fig. 2a,b display simulated current densities and temperature distributions, respectively, in a horizontal cross-section of the OLED stack in dependence of the total current. For increased total current they show strong spatial inhomogeneities which can be observed in Fig. 2c,d showing a cut along the symmetry line of the horizontal cross-section. For comparison, a purely isothermal simulation is added in Fig. 2c,e.

The global NDR behavior, as observed in the S-shaped characteristics in Fig. 1 (right), has its origin in the appearance of local NDR zones in the organic transport layers. In particular, our simulations

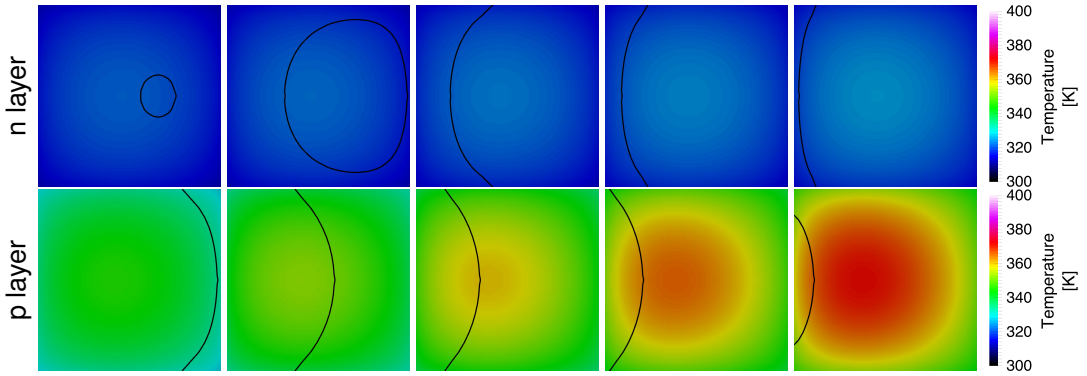

Figure 3: Propagation of local NDR zones in the OLED stack with increasing total current. The black lines indicate the sign change of the local differential resistance plotted over the temperature distribution. Top: behavior in the electron transport layer for the following values of the average current density: 265, 271, 279, 288, 298 mA/cm^2. NDR zone starts in a small region in the center and grows until it reaches the left contact. Bottom: behavior in the hole transport layer for average current densities 487, 553, 618, 679, 736 mA/cm^2. NDR starts at the right and moves to the left contact.

reveal a pronounced spatial propagation of local NDR zones for growing total current: Fig. 3 shows this effect in the electron transport layer (top) and the hole transport layer (bottom) for increasing total currents. The black lines represent the sign change of the local differential resistance plotted over the temperature distribution. It is clearly visible that NDR zones propagate laterally through the device starting in the electron transport layer for moderate total current, and eventually in the hole transport layer at higher total currents. But this effect did not appear in the recombination layer in our simulations. A propagation of local NDR zones was already observed in [FKG$^+$14] using electrothermal circuit simulations of large-area OLEDs. However, our PDE approach is far superior when multiple layers are considered, complex 3D substrate geometries are used, and special thermal environments are present. Moreover, it can be used to validate optimization strategies.

6 Conclusion

The complex behavior in organic devices, caused by temperature-activated conductivity in connection with Joule self-heating has been studied by 3D numerical simulation of a red OLED using a new PDE thermistor model. The S-shaped characteristics with regions of NDR, observed in measurements, are accurately reproduced by our simulations. The presented model allows to treat multi-layer structures with parallel running transport mechanisms in substructures and includes the diode-like behavior in the recombination zone. Moreover, it is capable of handling more complicated geometries including OLEDs on curved surfaces.

Assuming that effective material parameters such as power exponents, reference conductivities and activation energies are obtained from comparisons of experiments and simulations for small-area OLEDs, our PDE thermistor model allows us to predict the behavior of OLED devices of arbitrary size, such as large-area lighting panels. Moreover, the model can be used to transfer results from computational material science, e.g. via kinetic Monte Carlo simulations of OLED layers (see [KvdHH$^+$15]), to estimate the performance of OLED devices under self-heating conditions.

It turns out that strong electrothermal feedback will be the key to design uniform and stable OLEDs in future. The general understanding will also help to predict and improve long-term stability of OLEDs

driven at very high current densities, e.g. as planned in the automotive industry.

References

[BGL16] M. Bulíček, A. Glitzky, and M. Liero. Systems describing electrothermal effects with $p(x)$-Laplace like structure for discontinuous variable exponents. *SIAM J. Math. Analysis*, 48:3496–3514, 2016.

[BH08] A. Bradji and R. Herbin. Discretization of coupled heat and electrical diffusion problems by finite-element and finite-volume methods. *IMA J. Numer. Anal.*, 28(3):469–495, 2008.

[BK11] H. Bässler and A. Köhler. Charge transport in organic semiconductors. In *Unimolecular and supramolecular electronics I*, pages 1–65. Springer, 2011.

[FGL17] J. Fuhrmann, A. Glitzky, and M. Liero. Hybrid finite-volume/finite-element schemes for $p(x)$-Laplace thermistor models. In C. Cancès and P. Omnes, editors, *Finite Volumes for Complex Applications VIII - Hyperbolic, Elliptic and Parabolic Problems: FVCA 8, Lille, France, June 2017*, pages 397–405. Springer International Publishing, Cham, 2017.

[FKG+14] A. Fischer, T. Koprucki, K. Gärtner, J. Brückner, B. Lüssem, K. Leo, A. Glitzky, and R. Scholz. Feel the heat: Nonlinear electrothermal feedback in organic LEDs. *Adv. Funct. Mater.*, 24:3367–3374, 2014.

[FPL+13] A. Fischer, P. Pahner, B. Lüssem, K. Leo, R. Scholz, T. Koprucki, K. Gärtner, and A. Glitzky. Self-heating, bistability, and thermal switching in organic semiconductors. *Phys. Rev. Lett.*, 110:126601/1–126601/5, 2013.

[GL17] A. Glitzky and M. Liero. Analysis of $p(x)$-Laplace thermistor models describing the electrothermal behavior of organic semiconductor devices. *Nonlinear Anal. Real World Appl.*, 34:536–562, 2017.

[KAH+17] C. Kirsch, S. Altazin, R. Hiestand, T. Beierlein, R. Ferrini, T. Offermans, L. Penninck, and B. Ruhstaller. Electrothermal simulation of large-area semiconductor devices. *The International Journal of Multiphysics*, 11(2), 2017.

[KvdHH+15] P. Kordt, J. J. van der Holst, M. Al Helwi, W. Kowalsky, F. May, A. Badinski, C. Lennartz, and D. Andrienko. Modeling of organic light emitting diodes: From molecular to device properties. *Advanced Functional Materials*, 25(13):1955–1971, 2015.

[LKF+15] M. Liero, Th. Koprucki, A. Fischer, R. Scholz, and A. Glitzky. p-Laplace thermistor modeling of electrothermal feedback in organic semiconductor devices. *Z. Angew. Math. Phys.*, 66:2957–2977, 2015.

[SBH+11] M. Slawinski, D. Bertram, M. Heuken, H. Kalisch, and A. Vescan. Electrothermal characterization of large-area organic light-emitting diodes employing finite-element simulation. *Organic Electronics*, 12(8):1399–1405, 2011.

[SSMM+13] T. Schwab, S. Schubert, L. Müller-Meskamp, K. Leo, and M. C. Gather. Eliminating micro-cavity effects in white top-emitting OLEDs by ultra-thin metallic top electrodes. *Advanced Optical Materials*, 1:921–925, 2013.